AN APPROXIMATE DAMAGE MODEL FOR CONCRETE UNDER FINITE DEFORMATION

S. Khajehpour[1], G.D. Morandin and R.G. Sauvé

Computational Mechanics Development
Reactor Engineering Services
Atomic Energy of Canada Ltd.
2251 Speakman Dr.,
Mississauga, On, Canada L5K 1B2

Abstract

As the computing power of computers is constantly increasing, more accurate finite element analysis and detailed modelling of structures are sought. The critical issue of concern at hand is the characterization of complex material constitutive behaviour using numerical techniques. Finite element analysis of reinforced concrete structures under severe and reversible loadings requires a proper representation of concrete material behaviour. Abnormal loads such as impact, blast and seismic are generally reversible and cause structures to vibrate. To arrive at a reasonable approximation of damage in reinforced concrete structures under abnormal loading, the cracking of the concrete and its direction must be addressed. The inclusion of a mechanism that accounts for crack closure should be considered to include the compression strength of the cracked concrete if the load direction is reversed and the crack is closed. Thus, development of an improved material model for concrete and its implementation in a non-linear finite element code that is well suited to this class of problem is undertaken. In the work described in this paper, the methodology used in the development of this new material model for concrete is discussed. A sample case is analysed and the results of these FE analyses are discussed. The new concrete material model predicts the location and the direction of the cracks accurately and also allows for the inclusion of the compression strength of the cracked material in directions parallel to crack plane. In addition the closure of the crack and re-activation of the compression strength of the concrete orthogonal to the crack plane when the crack is closed is achieved.

1. Introduction

The work described in this paper covers the methodology used to evaluate the structural integrity of a reinforced concrete structure (shown in Figure 1) following a postulated handling accident scenario. To achieve this objective, a material model that approximately represents true behaviour of concrete material is developed. The primary structure considered in this work will be used for the purpose of facilitating the loading of a special container with radiated waste material. It is postulated that during the various handling operations, a loading accident occurs when the container is suspended over the structure at a certain vertical position above the water surface. The objective of this work is to determine, using full-scale explicit transient analysis with modelling of reinforced concrete, if the mentioned reinforced structure is capable of withstanding the pressure pulse generated by the accidental drop of the container onto the surface of the water contained in the loading bay. The loading considered in this work arises from dropping the container from the maximum handling height of 0.354 m onto the surface of the water assuming that the concrete structure is filled with water. This evaluation was achieved by employing the concrete material model described in this paper as part of the state-of-the-art three-dimensional non-linear continuum computer code H3DMAP (Sauvé, R.G. et al. 2004) for the numerical simulation of the fluid-structure interaction response of the container drop-generated shock wave. Pertinent modelling details include the hydrodynamic and acoustic

[1] khajehpours@aecl.ca, Corresponding author

M. Pandey et al. (eds), Advances in Engineering Structures, Mechanics & Construction, 87–98.

effects of the fluid with surface waves, discrete attachments, finite deformation material constitutive laws (i.e., large displacement and large strain), concrete reinforcing bar and large motion sliding/contact surfaces between the water and containing structures. Description of the proposed concrete material model, the method of analysis, key assumptions, and detailed results are presented in this paper.

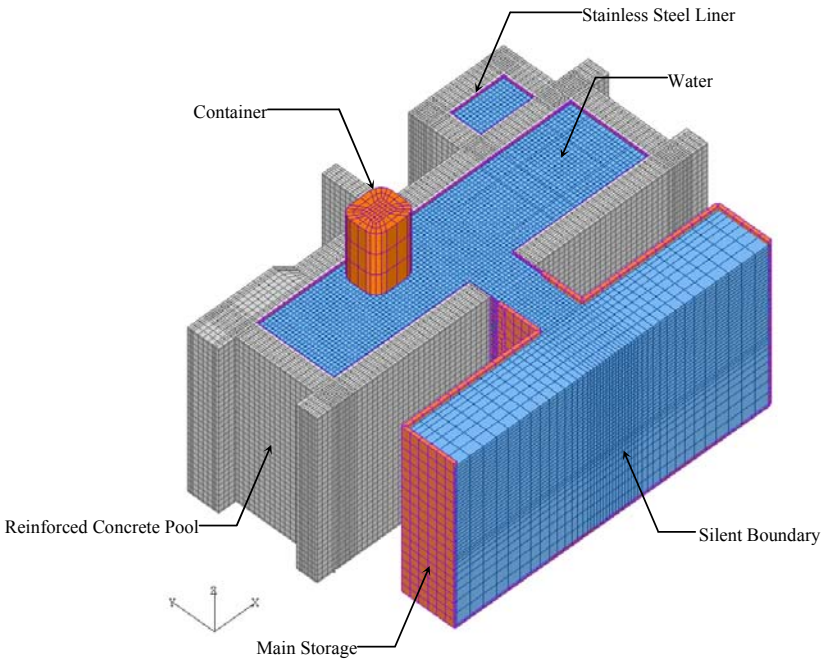

Figure 1: Overall View of Reinforced Concrete Structure (FE Model)

2. Methodology for Inclusion of Cracks in Concrete Material Model

The major methodologies used in finite element modelling of fracture in material are namely: a) the discrete and b) the smeared approaches (Gerstle W, et al.). In a smeared model, cracks are represented by changing the constitutive properties of the finite elements rather than changing the topography of the finite element meshing (Rashid) whereas the discrete model treats a crack as a geometric entity (Ngo et al.). The material model proposed in this paper is based on the smeared methodology. To achieve an accurate representation of cracked concrete material, it is imperative that the cracked plane is established. The methodology for the proposed material model is employed to find the crack plane in an element based on the principal stresses at the instant that cracking in the element occurs. In dynamic problems, where structures experience large displacements, the relativity of the crack plane to the element axis must be preserved as the element is displaced in three-dimensional space. The steps necessary to account for cracking of an element and its displacement in three-dimensional space are briefly described in this section followed by a brief discussion on how the compression failure of concrete is considered.

In Figure 2, the sequences of steps taken to establish the fracture of each element is shown. The first step is to verify if the element of concern has been cracked in previous time steps. Depending on the crack status of the element the following steps are taken,

1. If the element has never cracked before:

a. The maximum principal stress is found to establish if element is under tensile normal stress,

b. If the maximum principal stress is greater than tensile strength of material then the Jacobi iterative method is used (Golub G. et al.) to find the rotation tensor that relates the global to principal axes. This tensor transforms the element stress tensor to the principal stress tensor (cracked plane stress tensor); the same tensor can be used to relate the cracked plane to the element axis,

c. The tensile principal stress that exceeds the tensile strength of material is set to zero (cracking has occurred); the stress perpendicular to crack plane is released and reapplied to the structure as residual loads,

d. The tensile strength of the material in the element is set to zero,

e. The Cracked and Ever-Cracked flags are activated,

f. The principal stress (tensile crack component removed) tensor is rotated back to the element axis using the rotation tensor from step "b",

2. If the element has cracked at any point during static or dynamic loading stages:

a. The rotation tensor from step "b" is updated by using an average element spin (rotational velocity of the element) tensor in each time step,

b. The updated rotation tensor is then used to rotate the stresses in the element axis to the cracked plane,

c. If stress perpendicular to the crack plane is positive (tensile) then the value of the stress in that direction is set to zero,

d. The crack plane stress (tensile removed) tensor is rotated back to the element axis using the rotation tensor from step "a",

e. The Cracked flag is activated.

When the status of the element regarding the crack is established, a compressive failure using a failure model as shown in Figure 3 is checked. Failure of the element is based on the element hydrostatic pressure and deviatoric stresses. For concrete, it is proposed to use a hydrodynamic pressure-dependent material model in conjunction with a failure/damage model. Since the reinforcing steel is explicitly modelled, the need for assumptions regarding the use of a mixture rule is avoided. In this proposed material model, a pressure-dependent flow rule is defined with the attendant parabolic form of the yield function for compression as:

$$\varphi = J_2 - [a_0 + a_1 p] \quad \textbf{(1)}$$

where p is the hydrostatic stress (pressure), J_2 is the second invariant of the deviatoric stress tensor, a_0 and a_1 are the constants that are defined based on the concrete material. At yield φ=0 and $J_2=\sigma_y^2/3$ where σ_y is the yield point corresponding to hydrostatic stress p in the concrete. The basic specification data for the concrete is obtained in references (Bangash, M.) and (Winter, G. et al.).

If J_2 is less than $[a_0+a_1p]$, then no compression failure in the element has occurred. In cases, when J_2 is slightly larger than $[a_0+a_1p]$, to account for a relatively small ductility in concrete, some ductility might be defined as a percentage of the yield (shaded area in Figure 3). For these cases the deviatoric stresses are scaled down using equation (2).

$$\beta = \frac{\sigma_y}{\sqrt{3J_2}} \quad \textbf{(2)}$$

If J_2 is significantly larger than $[a_0+a_1p]$, the element is considered failed in compression. Theoretically, as hydrostatic pressure increases, yield stress of the material increase. However, two cap models are considered to limit the extent at which the yield strength can be increased (Figure 3).

These cap models ensure that the material properties will degrade after it has experienced large hydrostatic pressures. This is necessary due to the fact that voids in concrete material collapse and micro cracks are formed in the material.

For reversible loadings such as blast or impact, it is important to limit the strength of the element after it has passed the softening hydrostatic pressure (location I on Figure 3) to the minimum value it experienced during the previous loading phases. As an example if an element experiences hydrostatic pressures up to the value of location II on Figure 3 and the elliptical cap model is chosen, then the yield strength of that element is limited to σ_{yl}. This mechanism will ensure that elements that have previously experienced softening in their material strength will not carry loads beyond their set limits.

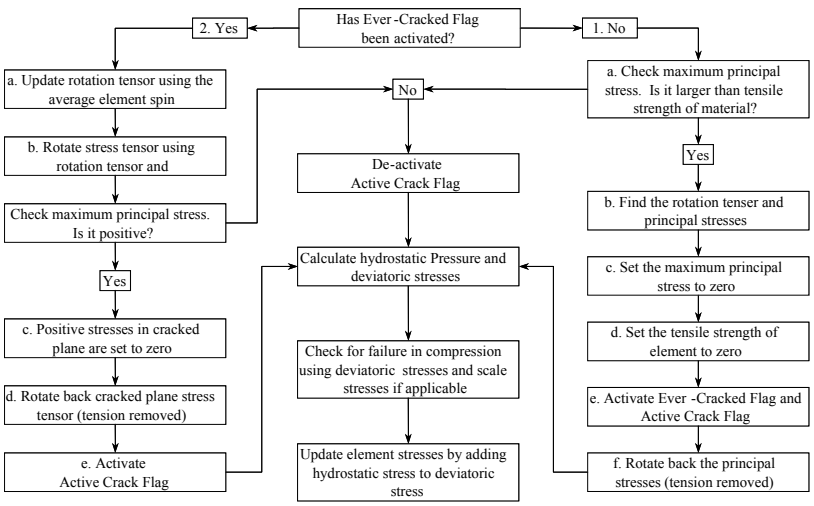

Figure 2: Methodology Flowchart

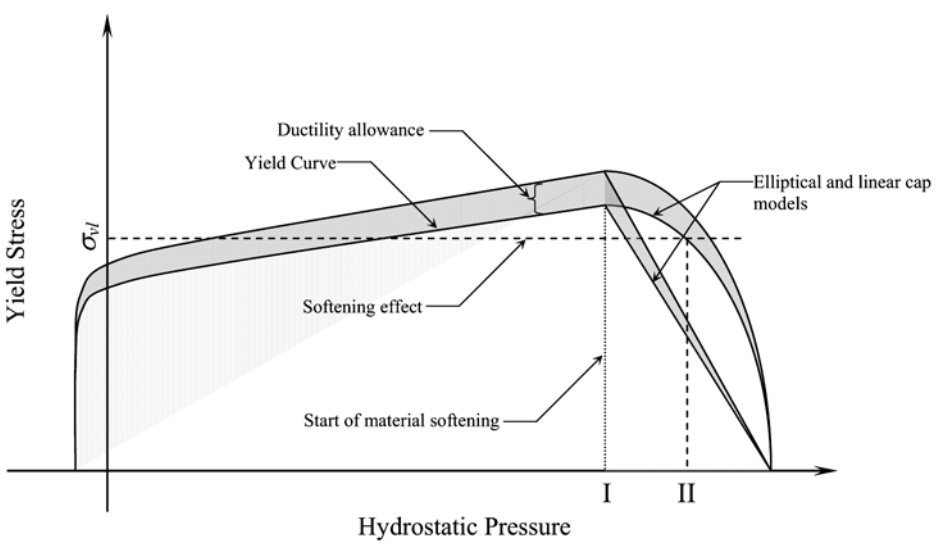

Figure 3: Yield Curve

An equation of state is employed for the proposed concrete material that relates the volumetric strain to the hydrostatic pressure in each element. This equation of state is used as part of the proposed material model in a form of a table lookup. The equation of state for the proposed concrete material is schematically shown in Figure 4.

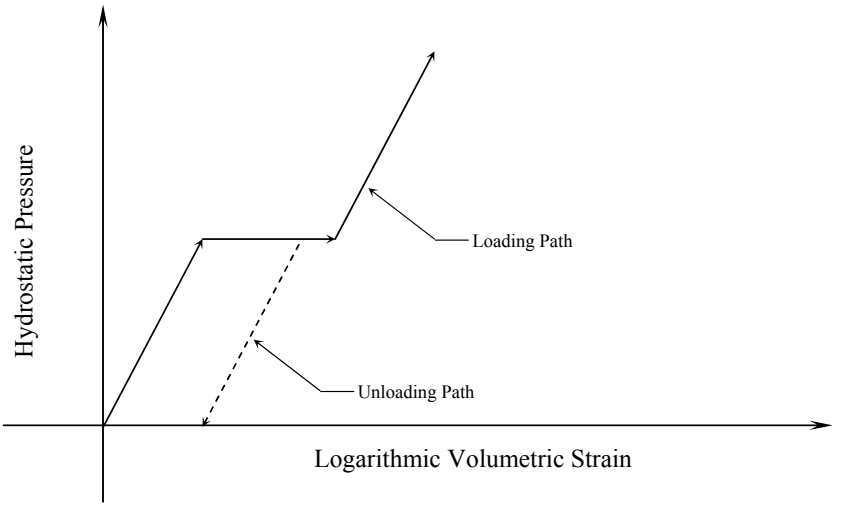

Figure 4: Equation of State

3. Example

The methodology described in Section 2 is employed for an assessment of a postulated accident scenario. The work described in this paper covers the methodology used to evaluate the integrity of the structure shown in Figure 1 following a postulated handling accident scenario. As described in Section 1, it is postulated that during the various operations, a loading accident occurs when the container is suspended at a certain vertical position above the water surface. The objective of this work is to determine, using full-scale analysis, if the reinforced concrete pool and neighbouring structures are capable of withstanding the pressure pulse generated by the accidental drop of the container onto the surface of the water contained in the pool.

3.1 Finite Element Model Description

In the analysis of the structure, a three-dimensional non-linear transient fluid-structure shock wave analysis is carried out to assess the structural integrity of the reinforced structure following a postulated handling accident. In Figure 1, the schematic representation of the structure of intent and part of the surrounding structures are shown. Given the localized nature of the drop scenario considered, only part of the water in the adjacent structure is included in the assessment as shown in Figure 1. Since the main storage is not directly connected to the pool, it is modelled using rigid shell elements. To ensure that the main storage contribution to the lateral stability and rigidity of the adjacent pool is minimized, the channel that connects the main storage to the pool is modelled in a manner that will minimize the transfer of load to the pool. The discretised components of the full model are shown Figure 1. The embedded reinforcing bars are explicitly modelled considering their respective diameters. The reinforcing bar topology is shown in Figure 5.

Given the complexity of the model, a variety of element types are used for each of the structural components and are listed in Table 1. In addition to the non-linear structural components, the water transmitting the shock wave within the containing structure is modelled using a hydrodynamic finite element formulation. The fluid-structure interaction is accommodated using a large deformation contact/sliding surface algorithm applied to all fluid-structure boundaries. At the boundary interfaces

of the main storage structure and fluid, silent (i.e., non-reflective) viscous elements are utilized. This prevents artificial wave reflections due to modelling constraints by permitting incident waves to travel through the boundary to the portion not included in the model.

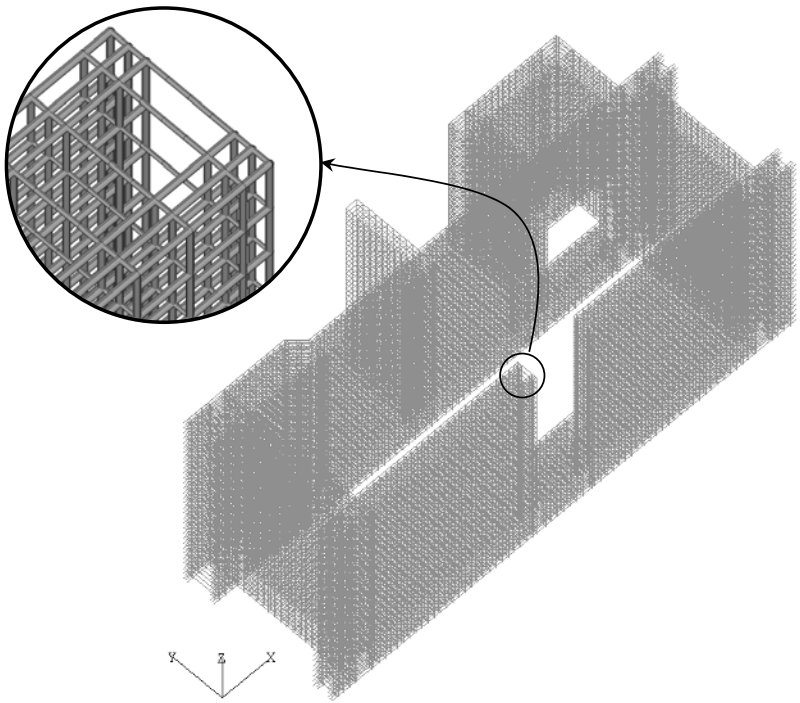

Figure 5: Steel Reinforcement in Wet Cask Handling Bay

Table 1 Details of Simulation Model Topology

Model Details		
Component	**Element Type**	**Number of Elements**
Concrete	3D Continuum	86,408
Rebar	3D Beam	132,422
S.S. Steel Liner	3D Shell	7,138
Inspection Platform	3D Shell	4,648
Inspection Platform	3D Beam	5,712
Water	3D Continuum (Hydrodynamic)	133,456
Container	3D Continuum (Rigid)	252
Bottom of the main storage and pool	3D Shell	2,572
Contact Pairs	Contact	6
Total Number of Elements		372,614
Total Number of Nodal Points		254,576

3.2 Material Model

Details of the material input data, used to model each of the components outlined in Table 1, are given in the following:

3.3 Concrete

The coefficients are obtained to give yield stress versus pressure consistent with values given for concrete with $f_C^{'} = 25\ MPa$ in the literature (Bangash, M.) and (Winter, G. et al.). In the event of failure, the concrete material is permitted to fail around the reinforcing bar. The specific data for the concrete used in the analysis is listed in the following.

Compressive strength $f_c^{'}$	= 25 MPa
Weight per unit volume	= 2400 kg/m^3
Modulus of Elasticity	= 23,400 MPa
Shear modulus	= 10,174 MPa
Poisson's ratio	= 0.15
Modules of rupture (tensile strength) f_r	= 2.5 MPa
Cracking Failure Criterion	= principal stress > f_r /3
Pressure-hardening yield function:	$\varphi = \sigma_y^2 - [226.5 + 29.2p]$

3.4 Reinforcing Steel

The reinforcing bars are explicitly modelled (Figure 5). The diameters of the bars are included as per the specification.

Weight per unit volume	= 7800 kg/m^3
Modulus of Elasticity	= 200,000 MPa
Poisson's ratio	= 0.3
Initial yield strength	= 400 MPa
Hardening Modulus	= 0.0 (elastic-perfectly plastic).

3.5 304L Stainless Steel Liner (5 mm) and Inspection Platforms

For this material, a bi-linear elastic-plastic isotropic hardening model is applied. This material model is applicable to finite deformation and calculated on a co-rotational material frame in the beam and shell elements. This provides for objectivity in the updated configuration. Shell thinning is included and failure of the liner plate structure is defined when the maximum plastic strain is exceeded at all the fibres through the thickness of the shell. Three integration points through the thickness are used to sample the non-linear response and obtain the thinning. For HSS beam members, sixteen integration points around the cross section of the member is used to capture the non-linear response of the beam members. Weight per unit volume = 7800 kg/m^3

Modulus of Elasticity	= 200,000 MPa.
Poisson's ratio	= 0.3
Initial yield strength	= 170 MPa
Hardening Modulus	= 2000 MPa

3.6 Water

The water is modelled using a hydrodynamic formulation with an equation of state (Sauvé R.G. et al. 2004). Shock discontinuities at the shock front are handled using an adaptive bulk viscosity treatment that correctly spreads the shock over a number of elements as a propagated steady wave and eliminates the numerical noise associated with this type of analysis.

Mass per unit volume	= 1000 kg/m^3
Bulk Modulus	= 2071 MPa.

3.7 Loading Conditions

The loading on the model occurs from 1) hydrostatic/dynamic pressure of water and 2) the interaction of the container with the water at the water-container interface. The nodes defining the rigid container model impact the water surface with an impact velocity V_0, determined from rigid body mechanics:

$$V_0 = \sqrt{2gh} \tag{3}$$

Where h is the drop height and g is the gravitational constant.

The relative location of the container to the pool walls and loading platforms are given in Figure 6. The topological information of the drop is given in the following.

Weight of container	= 80 metric ton
Drop Orientation in Pool	= bottom down flat end
Distance of container from pool short wall	= 3.52 m
Distance of container from pool long Wall	= 1.05 m
Drop height above water surface, h	= 0.354 m
Impact velocity from (3)	= 2.64 m/s

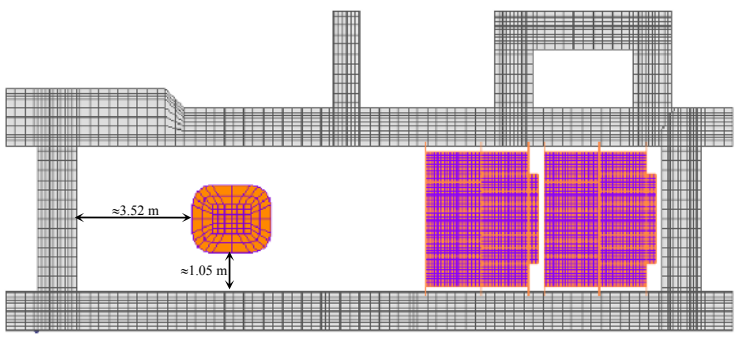

Figure 6: Plan view of Reinforced Concrete Structure

4. Assumptions

The key assumptions made in the simulation are as follows:

i) Given the localized nature of the drop scenario considered, only part of the water in the main storage in the proximity of the pool is included in the assessment. Since the water mass in the main storage is relatively large, a silent (non-reflective) boundary as shown in Figure 1 ensures that erroneous reflective waves are not included in the simulation.

ii) Since the main storage is not directly connected to the pool the main storage is modelled using rigid shell elements.

iii) To ensure that the main storage's contribution to the lateral stability and rigidity of the adjacent pool concrete wall is minimized, the channel that connects the main storage to the pool is modelled in a manner that will minimize the transfer of load to the pool. This is warranted, as the pool is not connected to the main storage.

iv) Failure in the concrete occurs when the principal stress exceeds a fraction (1/3) of the maximum tensile stress for the concrete material. This assumption ensures that the final results are conservative and no extra credit is given to concrete tensile strength.

v) Failure is assumed to occur in the stainless steel components and reinforcing rebar when the material continues to flow plastically beyond a specified effective plastic failure strain.

vi) No damping is assumed. The material's hysteresis arising from the non-linear response and failure provides the damping.

vii) It is assumed that the stainless steel liner is flush against the pool's concrete wall. The stainless steel liner is modelled explicitly to include its effect on the transfer of the shock wave from the

water to the reinforced concrete wall. However, it is prevented from contributing to the pool's rigidity and lateral stability.

viii) Inspection platforms are modelled with beam and shell elements that interact with water elements through common nodes. This ensures that the deformation of the platforms due to shock wave and water movement is conservatively captured.

5. Method of analysis and Results

The coupled fluid-structure model for the intended application must account for non-linear geometric and material behaviour. This includes elastic as well as finite deformation elastic-plastic constitutive laws for both three dimensional continuum and thin shells. The explicit solution module of the general-purpose, three-dimensional, non-linear in house finite element code H3DMAP (Sauvé R.G. et al. 2004) is used to simulate the shock wave propagation and resulting structural response. This module is based on the explicit hydrodynamic finite element formulation and includes the conservation of mass, momentum and energy equations. The element technology accounts for finite deformation (large displacement and strain) and includes shell thinning along with finite elastic-plastic materials and hydrodynamic material formulations. The efficiency and robust nature of the associated element technology and explicit algorithms make it particularly well suited to this class of stress wave propagation problem. The shell element is based on a co-rotational formulation that accounts for non-linear variations in through-thickness strains and large deformation (Sauvé R.G. et al. 1995). It is compatible with an under-integrated, eight-noded, three dimensional continuum element that includes a unified stabilization algorithm. A three-dimensional sliding/contact algorithm (Sauvé R.G. et al. 2005) provides the capability for modelling sliding interfaces with friction including interpolation of applicable quantities such as fluid forces and structural motions along a prescribed fluid-solid interface. A variety of failure models are used in conjunction with an erosion model that provides adaptive element deletion when element/material failure is detected.

The simulation is run to 800 millisecond (ms) beyond the initial impact at which time all pressure waves and dynamic effects resulting from the initial drop of the container onto the water surface are essentially dissipated. At approximately 10 to 15 ms after the impact, the initial shock wave is dissipated and the container is displacing the water in the pool as it descends. Initially a shock wave, imparted to the water, occurs under the container. A comparison of the pressure in the water, at a location in the centre of the container/water interface at the instant following the initial impact, with the peak pressure obtained from an idealization of the shock wave (i.e., water hammer) provides a useful, albeit approximate, check on the results of the simulation. Just following the initial drop, and before dissipation of the initial shockwave inspection of the peak pressure at the interface is predicted to be 3.95 MPa (shown in Figure 7). This compares to the peak value of 3.81 MPa obtained from the idealized acoustic wave equation.

In order to effectively track any damage to the containing structure during the course of the container drop generated pressure pulse, irrecoverable state variables such as cracking and effective plastic strain are stored at specified time intervals throughout the transient. In Figure 8 the crack locations in the concrete are identified before impact (under sustained hydrostatic load). As observed, localized cracking in the surface elements occurs in the concrete at the junction of the wall/wall and wall/foundation for the unsupported wall. These areas, being corners (wall to wall and wall to foundation), are subject to higher bending moments and hence higher tensile stress. In Figure 9 the locations where concrete has been cracked at least at one point in time during the simulation are shown. No crack on the outside surface of the pool concrete wall due to the pressure pulse generated by the drop is observed. Also from Figure 9, it is concluded that the cracks shown in Figure 8 marginally grow due to the impact-induced shock wave. It should be noted that since no plastic strain in the reinforcing rebar is observed as a result of the shock wave, the state of cracking in concrete after the shock wave would be the same as that shown in Figure 8 (i.e., tensile cracks due to the shock wave will close).

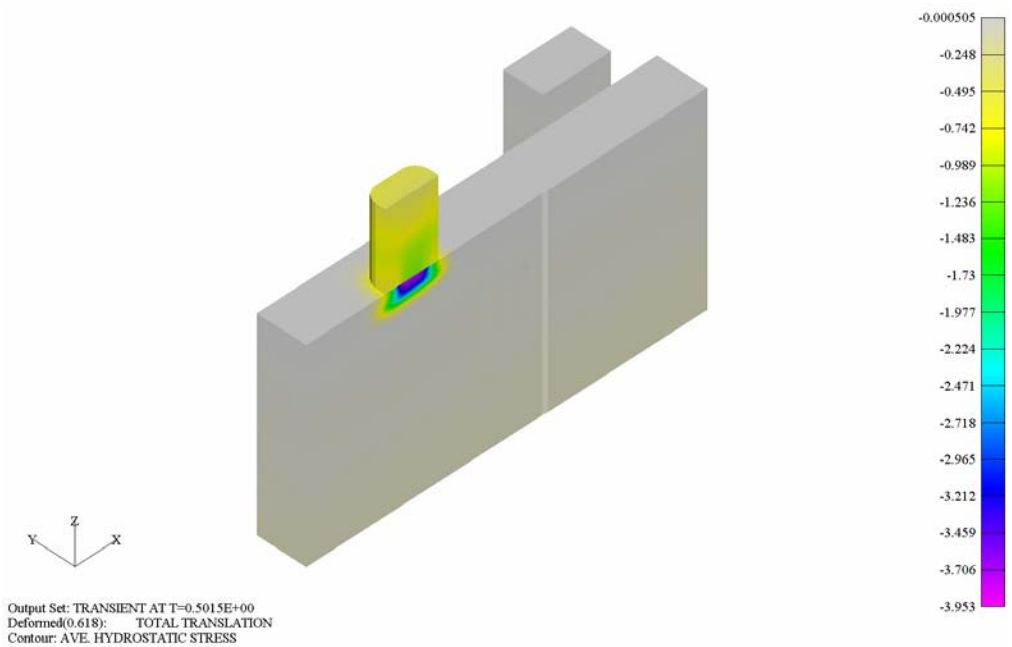

Figure 7: Hydrostatics Pressure in Water at Impact

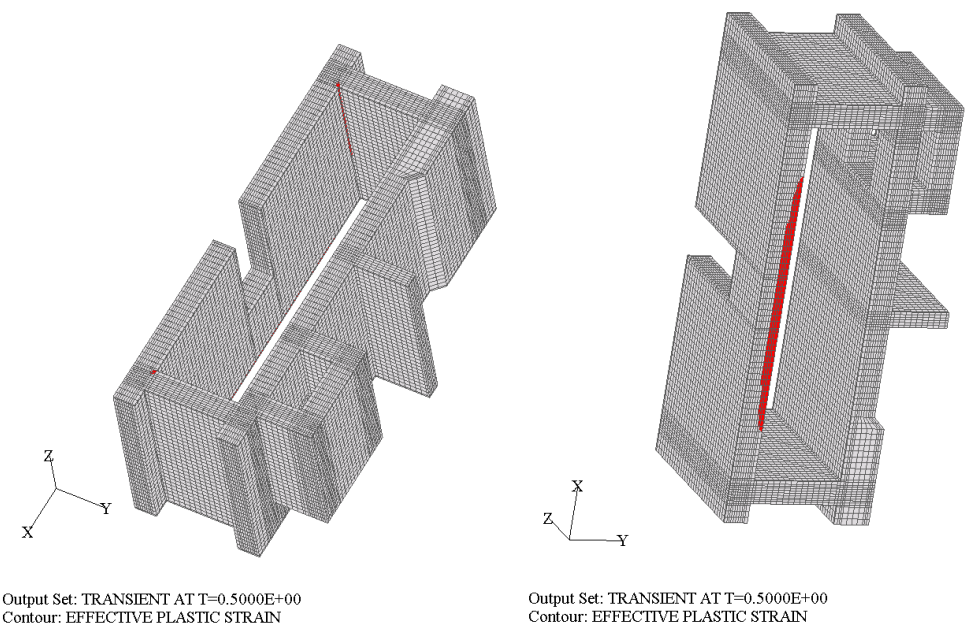

Figure 8: Accumulated Cracking in Concrete Before Impact

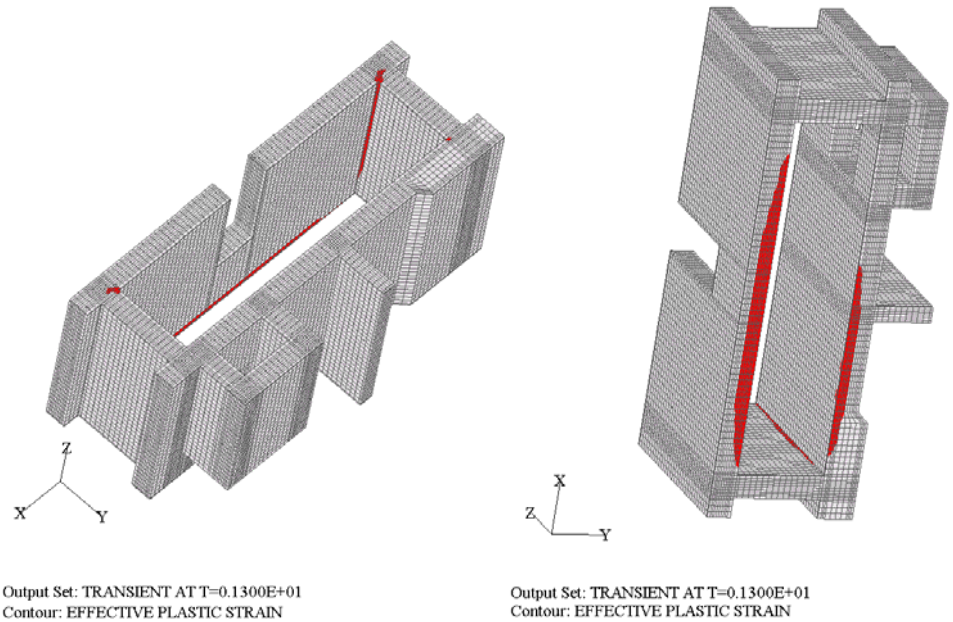

Figure 9: Accumulated Cracking in Concrete at End of Simulation

6. Conclusions

A simulation of a postulated container handling accident into a pool has been performed. The results indicate that for this accident scenario, no significant cracking of the concrete structure occurs due to the fluid shock wave propagation. While the stainless steel liner experiences virtually no damage and maintains its function, some localized cracking in the concrete is observed in the walls of the pool at the wall/wall and wall/foundation junctions. However, these cracks are a result of the sustained loading (hydrostatic water pressure) with some general and reversible increased crack widths and depths due to shock wave. There is no indication of plasticity in the rebar used in the reinforced concrete walls or in the inspection platforms. The material model described in this paper in conjunction with explicit finite element engines can be used to track the fracture of concrete material and will help analysts in prediction of damage level to reinforced concrete structures subjected to abnormal loadings.

References

Bangash, M.Y.H., 1989, *Concrete and Concrete Structures*, Elsevier Applied Science.

Gerstle W., et al., "Finite Element Analysis of Fracture in Concrete Structures: State-of-the-Art", ACI 446.3R-97.

Golub Gene H. and Van Loan Charles F., 1989, *Matrix Computations*, Second Edition, Johns Hopkins University Press.

Ngo, D. and Scordelis, A.C., 1967, "Finite Element Analysis of Reinforced Concrete Beams", *ACI Journal*, Proceedings Vol. 64, No. 3, March.

Rashid, Y.R., 1968, "Ultimate Strength Analysis of Prestressed Concrete Pressure Vessels", *Nuclear Engineering and Design*, Vol. 7.

Sauvé, R.G. and Metzger, D., 1995, "Efficient Unified Hourglass Stabilization for One Point Quadrature Three Dimensional Shell Elements'', In: Cory JF, Gordon JL, editors. *Current Topics in Computational Mechanics*, ASME PVP-305; pp. 3−10, July.

Sauvé, R.G. and Morandin, G., 2004, Computer Program Documentation – User Manual, Programmer Manual, H3DMAP Version 7: A Three Dimensional Finite Element Computer Code for Linear and Nonlinear Continuum Mechanics, AECL Report No. CW-114515-225-001 R0, May.

Sauvé, R.G. and Morandin, G.D, 2005, "Simulation of Contact in Finite Deformation Problems − Algorithm and Modelling Issues", *International Journal of Mechanics and Materials in Design*, Vol. 1, pp. 287−316.

Westbroke, H., 1990, "Hydrostatic Pressure Testing of Samples from the Concrete Integrated Container", Ontario Hydro Research Department, December.

Winter, G. and Nilson, A., 1979, *Design of Concrete Structures*, McGraw-Hill.